Paper No. 600

ESTIMATION OF PASSENGER VEHICLE INERTIAL PROPERTIES AND THEIR EFFECT ON STABILITY AND HANDLING

January 8, 2003

R. Wade Allen
David H. Klyde
Theodore J. Rosenthal
David M. Smith

Estimation of Passenger Vehicle Inertial Properties and Their Effect on Stability and Handling

R. Wade Allen, David H. Klyde, Theodore J. Rosenthal, David M. Smith

Systems Technology, Inc.

ABSTRACT

Vehicle handling and stability are significantly affected by inertial properties including moments of inertia and center of gravity location. This paper will present an analysis of the NHTSA Inertia Database and give regression equations that approximate moments of inertia and center of gravity height given basic vehicle properties including weight, width, length and height. The handling and stability consequences of the relationships of inertial properties with vehicle size will be analyzed in terms of previously published vehicle dynamics models, and through the use of a nonlinear maneuvering simulation.

INTRODUCTION

This paper generally analyzes how vehicle inertial properties (i.e., weight, moment of inertia and center of gravity location) relate to typical dimensions (length, width and height) and how these properties affect vehicle dynamics. It is useful to have a general appreciation of the effects of vehicle properties on stability and handling. This information is helpful in the preliminary phases of vehicle design, and should also be considered in after-market recommendations such as tire selection and vehicle loading. This paper takes advantage of an extensive database of inertial data provided by NHTSA (1) for a range of vehicles including passenger cars, vans, pickup trucks, and SUVs. Useful relationships between typical dimensions and inertial properties are provide through the use of regression analysis.

Inertial properties have known effects on vehicle dynamic response, and some of these relationships are discussed in this paper. Key inertial variables relate to directional and roll mode stability issues. A validated nonlinear simulation is used to demonstrate stability problems related to inertial properties. There is some indication from rollover accident analysis that vehicle size seems to be a contributing factor. The analysis herein attempts to uncover the inertial and/or size variables that might make small vehicles more vulnerable to stability problems than large vehicles.

The paper starts off with some background on basic vehicle dynamics analysis, and reanalysis of a prior accident database. The NHTSA Inertia Database [1] is then analyzed with regression analysis to reveal the relationships between vehicle inertial properties and basic size dimensions. Finally, we carry out some nonlinear computer simulation analysis with detailed vehicle models to show how size and speed interact to create stability problems.

BACKGROUND

Basic vehicle dynamics have been traditionally subdivided into lateral/directional dynamic modes including yawing and rolling motions [2]. The basic input for these dynamics is steering, and speed is a key operating point. Lateral/directional dynamics are affected significantly by inertial properties including mass, moments of inertia and cg (center of gravity) location as will be analyzed subsequently. Inertial properties affect the time constants of various response modes, and also the influence of control inputs.

Maneuvering can excite lateral/directional dynamics including the yaw and roll modes. Limit performance maneuvering (i.e. involving tire saturation) can lead to oversteer and high slip angles. High slip angles result in high lateral acceleration which provides input to the roll mode. Transient response including high lateral acceleration can lead to tip-up. Let us first consider some basic properties of lateral/directional dynamics. Then we will consider the roll divergence time constant involved in the dynamics of tip-up. Finally, we will review some evidence for the influence of vehicle size on rollover rates.

Lateral/Directional Stability

Previously published lateral/directional vehicle dynamics models give a general feeling for the effect of vehicle inertial properties on vehicle handling and stability. A bicycle model is summarized in [2] based on earlier work that includes the effects of inertial properties, tire properties and speed. The following matrix expresses vehicle lateral velocity (v) and yaw rate (r) as a function

of front wheel steering input (δ_w) in a Laplace transform formulation as follows:

$$\begin{bmatrix} s-Y_v & U_0-Y_r \\ -N_v & s-N_r \end{bmatrix} \begin{bmatrix} v \\ r \end{bmatrix} = \begin{bmatrix} Y_{\delta_w} \\ N_{\delta_w} \end{bmatrix} \delta_w \qquad (1)$$

where s is the Laplace operator, the operating point speed is U_o, Y_v, Y_r, N_v, N_r are the stability derivatives and $Y_{\delta_w}, N_{\delta_w}$ are the control derivatives.

The stability and control derivatives are functions of the tire cornering stiffness (Y_{α_1} and Y_{α_2} respectively for the front and rear tires), and previous research [2, 3] has shown that load normalized cornering stiffness or cornering coefficient is relatively constant at a given load across tire size:

$$Y_\alpha^* = Y_\alpha / F_z$$

The per tire normal load F_z can be defined for each axle according to the longitudinal cg location where, $a =$ distance to front axle and $b =$ distance to rear axle:

Front Axle $\qquad F_{z_1} = bmg / 2(a+b)$

Rear Axle $\qquad F_{z_2} = amg / 2(a+b)$

Therefore, on a per tire basis for the front and rear axles respectively, where mg (mass x acceleration due to gravity) is the vehicle weight, we have:

Front Cornering Coefficient $\quad Y_{\alpha_1}^* = 2(a+b)Y_{\alpha 1} / bmg$

and $\qquad\qquad\qquad\qquad\qquad\qquad\qquad (2)$

Rear Cornering Coefficient $\quad Y_{\alpha_2}^* = 2(a+b)Y_{\alpha 2} / amg$

Now using these cornering coefficients, the bicycle model stability and control derivatives for the lateral and directional modes given in [2] can be expressed as follows:

Lateral

$$Y_v = -\frac{g}{U_0(a+b)}\left(bY_{\alpha_1}^* + aY_{\alpha_2}^*\right); \; Y_r = \frac{abg}{U_0(a+b)}\left(Y_{\alpha_2}^* - Y_{\alpha_1}^*\right);$$
$$Y_{\delta_w} = \frac{bg}{(a+b)}Y_{\alpha_1}^* \qquad (3)$$

Directional

$$N_v = \frac{abmg}{I_z U_0(a+b)}\left(Y_{\alpha_2}^* - Y_{\alpha_1}^*\right);$$
$$N_r = -\frac{abmg}{I_z U_0(a+b)}\left(aY_{\alpha_1}^* + bY_{\alpha_2}^*\right); \; N_{\delta_w} = \frac{abmg}{I_z(a+b)}Y_{\alpha_1}^* \qquad (4)$$

The transfer function of yaw rate to steering input is given by:

$$\frac{r}{\delta_w}(s) = \frac{N_{\delta_w}\left(s+1/T_r\right)}{\left[s^2 + Bs + C\right]} \qquad (5)$$

where

$$T_r^{-1} = \frac{g}{U_0}Y_{\alpha_2}^* \qquad (6)$$

$$B = -(Y_v + N_r) = \frac{g}{U_0(a+b)}\left[bY_{\alpha_1}\left(1+\frac{a^2}{k_z^2}\right) + aY_{\alpha_2}\left(1+\frac{b^2}{k_z^2}\right)\right] \qquad (7)$$

and

$$C = U_0 N_v + \left(Y_v N_r - Y_r N_v\right) = \left(\frac{g}{U_0}\right)^2 \frac{abY_{\alpha_1}^* Y_{\alpha_2}^*}{k_z^2}(1+KU_0^2) \qquad (8)$$

where $k_z = \sqrt{I_z/m}$ = radius of gyration about the body yaw or z-axis, and K is referred to as the stability factor and is proportional to the SAE understeer/oversteer gradient:

$$K_{SAE} \text{ (deg/g)}=1847 \; (a+b) \, K \; (\sec^2/\text{ft}) \qquad (9)$$

The stability factor K is defined in terms of the vehicle stability derivatives as:

$$K = \frac{N_v}{\left(Y_v N_r - Y_r N_v\right)U_0} = \frac{1}{g(a+b)}\left(\frac{1}{Y_{\alpha_1}^*} - \frac{1}{Y_{\alpha_2}^*}\right) \qquad (10)$$

Note that the bicycle model directional control and stability derivatives respectively (N_{δ_w}, N_v, N_r) are dominated by weight (mg), yaw moment of inertia(I_z), and speed (U_0) in addition to the tire properties ($Y_{\alpha_1}^*$ and $Y_{\alpha_2}^*$) while the lateral control and stability derivatives respectively (Y_{δ_w}, Y_v, Y_r) are independent of the inertial properties aside from the longitudinal weight distribution (i.e. a,b). Vehicle stability factor is also independent of inertial properties. Thus, small vehicles should be more responsive in yaw than larger vehicles both in terms of their response to control inputs (N_{δ_w}), and their transient response independent of the control input (Equations 7 and 8).

The matrix Equation 1 is essentially valid for linear perturbations about speed and tire cornering coefficient operating points. As has been presented previously [2] the tire coefficients are a function of lateral acceleration, the linear range of which extends up to on the order of 0.3 g's. Beyond this the tires go into increasing levels of saturation, and the cornering stiffness coefficients fall off. The essential effect of this is to increase the yaw rate time constant, decrease the bandwidth of the yaw rate transfer function, and limit lateral acceleration which degrades the lateral acceleration bandwidth. Furthermore, when the rear axle saturates before the front axle during maneuvering, the vehicle will go into transient oversteer and can potentially spinout [4]. These effects are all reasonably represented in a perturbation context in the above equations if the proper speed and tire cornering coefficient operating points are accounted for.

Roll Stability

Previous research has described the conditions that lead to tip-up, e.g. [4, 5]. Figure 1a) illustrates the basic condition that the maneuvering acceleration (tire forces) overcome the vehicle weight such that the composite force vector falls outside of the tire patch which leads to an overturning moment. This condition results in an unstable pendulum as illustrated in Figure 1b) which leads to an unstable divergence in the roll mode. This condition can be modeled by the following differential equation expressing Newton's law for rotational elements:
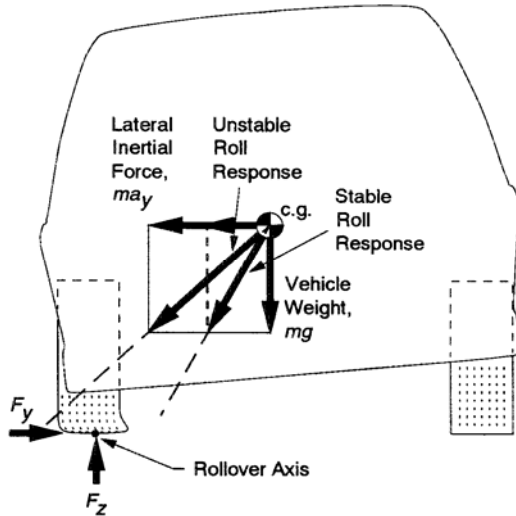
a) General Conditions for Maneuver Induced Tip-up.

$$I'_x = I_x + e^2 m$$
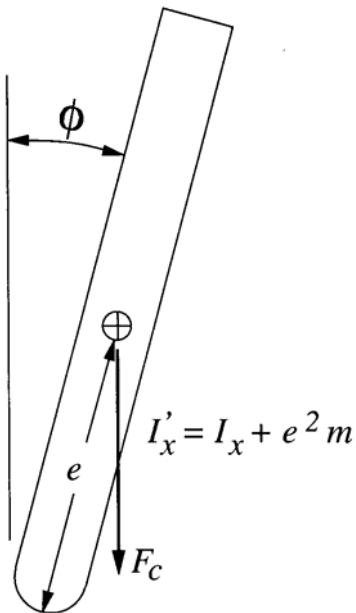
b) Equivalent Unstable Pendulum During Tip-up.

Figure 1. Conditions for Tip-up and Rollover

$$I'_x \frac{d^2\phi}{dt^2} = e\, F_c\, \phi \qquad (11)$$

Taking the Laplace transform and solving for the roots of the equation we have:

$$s \pm \sqrt{\frac{e\, F_c}{I'_x}} = 0 \qquad (12)$$

The above equation tells us that we have an unstable divergence time constant at:

$$T_d = \sqrt{\frac{I'_x}{e\, F_c}} \qquad (13)$$

The roll mode should diverge at this rate, and we see from the above expression that smaller vehicles (i.e. smaller I'_x) should have smaller (faster) time constants.

Accident Analysis

Analysis of accident rates also indicates some relationship to vehicle size. Given several analyses including and excluding the independent variables of wheelbase and static stability factor, Mengert [6] concludes that "a model with both stability factor and wheelbase predicts rollover significantly better than stability factor alone." Wheelbase was also found to be a significant factor in subsequent rollover research [5]. The rollover data base from this work (Appendix E) was reanalyzed using a log transform of both the independent and dependent variables:

$$Log\ RR = c_1 + c_2\ Log\ T_w/2H_{cg} + c_3\ Log\ W_t \qquad (14)$$

where :

RR = rollovers/single vehicle accident

c_1, c_2, c_3 = regression coefficients

$T_w/2H_{cg}$ = SSF (Static Stability Factor)

W_t = vehicle total weight

Weight was used here as an inertial variable related to the size variable of wheel base used in previous analyses. The regression analysis results are given in Table 1 which shows a statistically significant relationship between the dependent and independent variables. Here we see that rollover rate increases with smaller values of both SSF and Weight, and the relationship for both variables is statistically significant (i.e. $p<.01$). Figure 2 shows the actual rollover rate versus the regression predicted rollover rate. Here we see that the relationship is quite consistent for all four vehicle classes (cars, vans, pickups and SUVs) with the exception of one large passenger car that had an extremely low rollover rate. The static stability factor is the dominant explanatory variable, which is consistent with Mengert's work [6] and recent analyses conducted by the National Academy of Sciences [7].

Table 1. Rollover Rate Regression Analysis Based on Data Taken From (5)

Regression Statistics

Multiple R	0.83638963
R Square	0.69954762
Adjusted R Square	0.68373433
Standard Error	0.14229352
Observations	41

ANOVA

	df	SS	MS	F	Signif. F
Regression	2	1.791411896	0.895706	44.238	1.196E-10
Residual	38	0.769402908	0.020247		
Total	40	2.560814804			

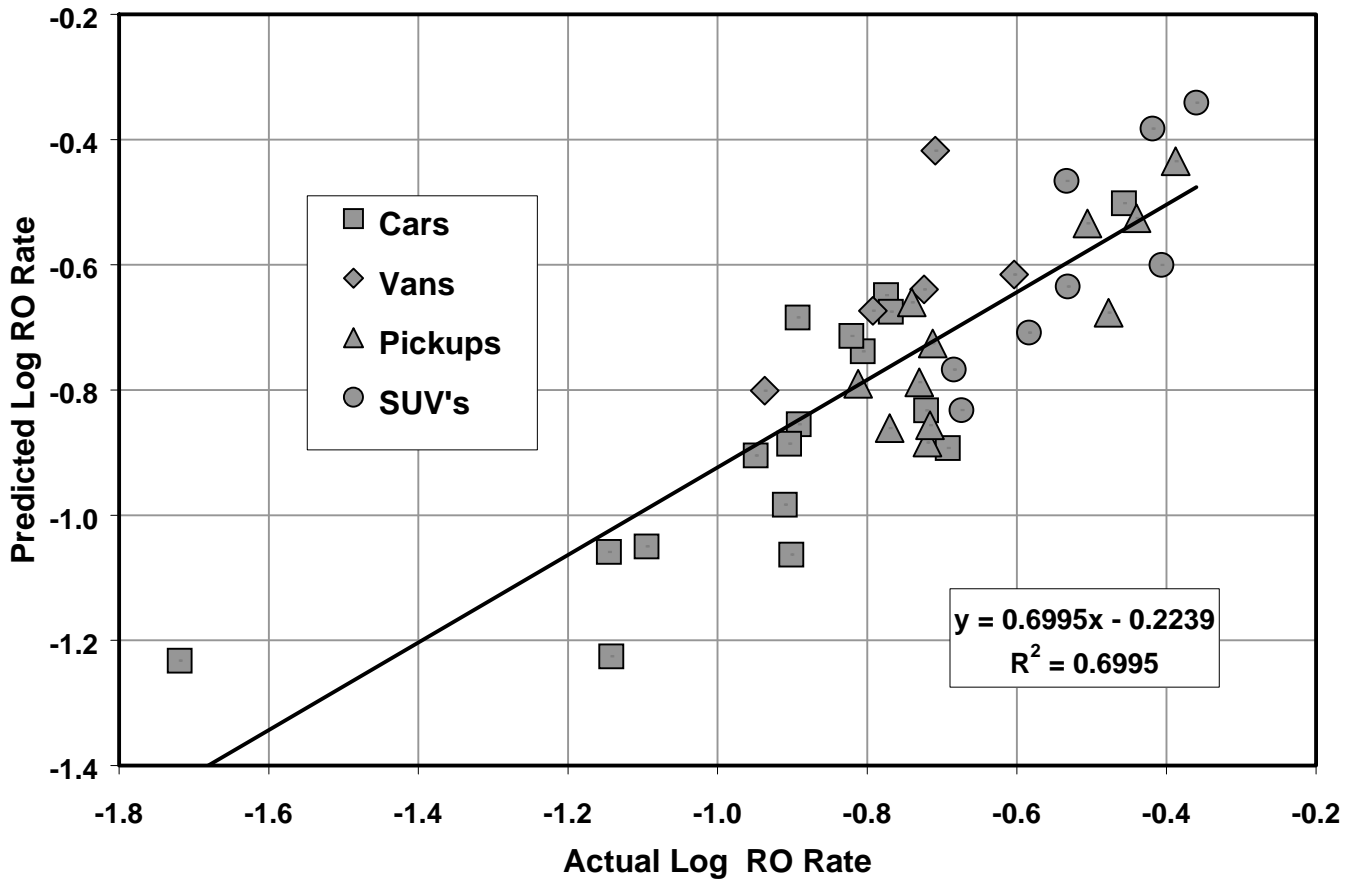|	Coefficients	Stand. Error	t Stat	P-value	Lower 95%	Upper 95%
Intercept	2.3727232	0.745568834	3.182433	0.00291	0.863398	3.8820485
Log $T_w/2H_{cg}$	-6.0502938	0.652265197	-9.275819	2.6E-11	-7.3707357	-4.7298519
Log W_t	-0.7621415	0.206098779	-3.697943	0.00068	-1.1793667	-0.3449163

Figure 2. Actual Versus Predicted RO Rates for Data from (5)

Taking the antilog of both sides of equation 14 gives the expression:

$$RR = 10^{c_1}\left(T_w/2H_{cg}\right)^{c_2} W_t^{c_3} \qquad (15)$$

This expression suggests that to maintain a given rollover rate, smaller vehicles should have higher static stability factors. It has been shown elsewhere [3] that the sensitivity of each of the independent regression variables is given by their coefficients:

$$\frac{d\,RR}{RR} = c_2 \frac{d\left(T_w/2H_{cg}\right)}{T_w/2H_{cg}} = c_3 \frac{d\,W_t}{W_t} \qquad (16)$$

Thus $T_w/2H_{cg}$ has a much greater influence on rollover rate than weight for the database taken from [5]. To get a more representative analysis of the relative influence of $T_w/2H_{cg}$ and weight, this analysis should be carried out for larger and more up to date databases with a more representative and larger cross section of vehicles. The analysis should also include demographics (i.e. age and gender) and environmental factors (i.e. road and weather conditions) to properly account for variables typically found to be significant in past accident analyses [6].

INERTIAL PROPERTIES

This analysis makes use of the NHTSA inertial data found on the NHTSA Web site (http://www.nrd.nhtsa.dot.gov/vrtc/ca/Cadata.htm) and described in [1]. Data were analyzed from rows 5 to 411

in the NHTSA spreadsheet file. Vehicles beyond row 411 had incomplete data. The first analysis to be considered is the relationship between moments of inertia and vehicle dimensions. As noted in Figure 3 the moments of inertia for a homogenous rectangular mass are products of mass and of dimensions length, width and height. Here we will assume that the moments of inertia of a vehicle are a general logarithmic function of key vehicle dimensions:

$$\begin{aligned} Log\, I_{x,y,z} = {}& Log\, k_1 + k_2 * Log\, l \\ & + k_3 * Log\, T_w + k_4 * Log\, H_r + k_5 * Log\, W_t \end{aligned} \qquad (17)$$

where

$I_{x,y,z}$	= principle moments of inertia
k_1	= constant of proportionality or intercept
k_2, k_3, k_4, k_5	= regression coefficients
l	= wheel base (feet)
T_w	= average track width (feet)
H_r	= roof height (feet)
W_t	= total weight (lbs)

Equation 17 is in a form that will allow multiple linear regression to be applied to the NHTSA inertial data base. Furthermore, if we take the antilogarithm of both sides of equation 1 we obtain the following expression for moment of inertia:

$$I_{x,y,z} = 10^{k_1} * l^{k_2} * T_w^{k_3} * H_r^{k_4} * W_t^{k_5} \qquad (18)$$
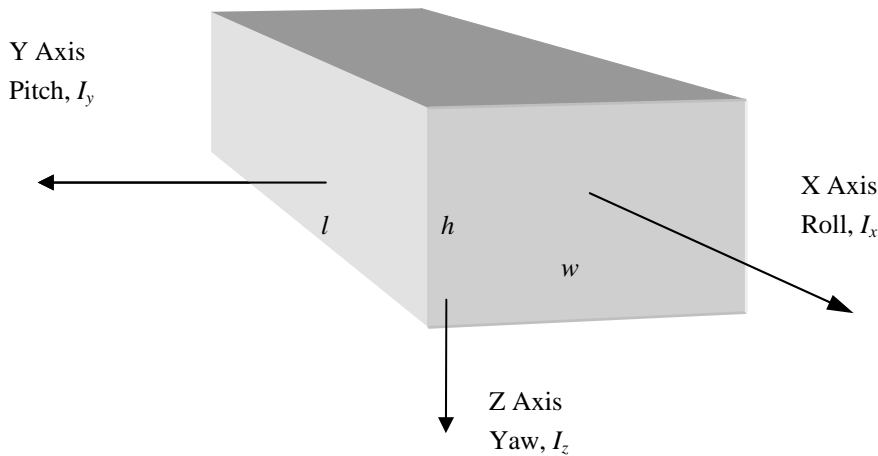
Roll Moment of Inertia: $I_x = \dfrac{1}{12}m\left(h^2 + w^2\right)$

Pitch Moment of Inertia: $I_y = \dfrac{1}{12}m\left(h^2 + l^2\right)$

Yaw Moment of Inertia: $I_z = \dfrac{1}{12}\left(w^2 + l^2\right)$

Figure 3. Moments of Inertia for a Homogeneous Mass.

Also, as described elsewhere [3], the sensitivity of each of the independent regression variables on moment of inertia is given by their coefficients. For example:

$$\frac{dI}{I} = k_2 * \frac{dl}{l} \qquad (19)$$

Regression analysis results are summarized for roll, pitch, and yaw moments of inertia in Tables 2 - 4. The regression correlations (r^2) are quite high, with the roll the lowest and yaw the highest. The contribution of each of the independent variables can be judged by the regression equation coefficients which indicate the percentage sensitivity contribution as described elsewhere [3], and also by the statistical significance parameter (i.e. an independent variable has a statistically reliable contribution when its 'p' value is less than 0.05). For roll moment of inertia (I_x) analysis in Table 2 the dominant contributions are made by track width and weight, while wheel base contributes the least. The pitch moment of inertia (I_y) analysis in Table 3 shows that wheel base and weight make the dominant contributions while roof height makes the least contribution as might be expected. For the yaw moment of inertia (I_y) analysis in Table 4 wheel base and weight make the major contribution while roof height is not statistically significant ($p > 0.05$).

If we were to take the moment of inertia equations in Figure 3 literally for a rectangular parallelepiped we see that weight (mg = mass x g) comes through with coefficients that are close to unity as expected. The multiplying constant should be Log (1/12g) = -2.59, but is somewhat less negative (i.e. a larger multiplying constant) in all three cases. Some differences specific to each of the axes are as follows:

Roll – The coefficient on the trackwidth (T_w) dimension is almost 2 as expected, but roof height has a small coefficient. This probably represents the wide variations in roof height between passenger cars and SUVs that does not represent much difference in moment of inertia. There is also a small negative coefficient on wheelbase (l) which decreases roll moment of inertia at longer wheel bases.

Pitch – Wheelbase is the dominant coefficient as expected, but is somewhat less than 2. Roof height is the second dimension in the pitch plane, but its effect is not statistically reliable ($p>.05$). Trackwidth (T_w) which is not in the pitch plane does have a statistically reliable, albeit small, effect.

Yaw – Both wheelbase (l) and trackwidth (T_w) are the yaw plane dimensions. Wheel base has a coefficient that is somewhat less than expected, while trackwidth has a significantly lower coefficient. The roof height coefficient is negligible, and not statistically reliable.

Figure 4 shows roll moment of inertia values versus the regression prediction. Here we see a relatively good correlation between the actual and predicted values for I_x with two significant outliers. The NHTSA database contains measurements for several examples of each vehicle, and the measurements for the outliers in Figure 4 and similar vehicles are indicated with different symbols. Here we see that different instances of the same vehicle give significantly different moments of inertia for roll. To a certain extent this indicates inherent variation in the measurements, although the highest and lowest outliers in Figure 4 (the circle and square) probably represent some measurement error.

Figure 5 and Figure 6 show actual versus predicted values of pitch and yaw moments of inertia respectively. Here we see that the regression predictions are quite reasonable, and that the variability is somewhat lower than that of the roll moment of inertia predictions in Figure 4. The ranges of the pitch and yaw moments of inertia are quite similar as might be expected since the mass distribution is similar in each case. In fact, if we consider the comparison of log pitch and yaw moments of inertia in Figure 7, we see that these two inertial properties are highly correlated. If we look back at the regression coefficients for the log pitch and yaw moments of inertia in Tables 3 and 4 we can see that they are also quite similar.

The above regression results could be influenced by generally high correlation between the various independent variables as might result from a pervasive size effect on all variables. This is not the case, however, as shown in the cross correlation matrix of Table 5. Here we see that the independent variables (i.e. WB, TW, RH and Wt) have high correlations with the dependent moments of inertia as might be expected, but much lower correlations within themselves. The moments of inertia have high correlations amongst themselves and with regard to weight, which is also to be expected.

The NHTSA database also includes cg (center of gravity) locations. Some percentage of roof height has often been proposed as an approximation for center of gravity location, e.g. [1, 5]. Figure 8 shows cg height as a function of roof height and the correlation is noted to be reasonable. The regression function in Figure 8 shows the proportionality factor to be about H_{cg} = 0.39 H_r. The longitudinal cg location determines front axle weight proportion which has been related to directional stability [5], i.e. a higher front weight distribution gives better directional stability. The distribution of front axle weight proportion is shown in Figure 9. Here we see that the median (50th percentile) vehicle has a weight distribution at the front axle of about 0.56. Half the vehicles have front axle weight distributions between 0.52 (25th percentile) and 0.60 (75th percentile), and about 83% of the vehicles have a front weight proportion of greater than 0.50.

The roll divergence time constant given by Equation 13 was computed for each vehicle in the NHTSA database. The composite force was assumed to be given by the vector of vehicle weight and lateral tipup force

Table 2. Regression Analysis Summary for Roll Moment of Inertia I_x

Regression Statistics	
Multiple R	0.95646
R Square	0.91481
Adjusted R Square	0.91396
Standard Error	0.04893
Observations	407

ANOVA

	Df	SS	MS	F	Signif. F
Regression	4	10.3354	2.5839	1079.25	1.87E-213
Residual	402	0.9624	0.0024		
Total	406	11.2979			

	Coefficients	Standard Error	t Stat	P-value	Lower 95%	Upper 95%
Intercept	-2.1363	0.07973	-26.793	1.83E-91	-2.2930	-1.9795
Log I	-0.1596	0.07742	-2.061	4.00E-02	-0.3118	-0.0073
Log T_w	1.9404	0.13957	13.902	3.73E-36	1.6660	2.2148
Log H_r	0.3629	0.06467	5.611	3.75E-08	0.2357	0.4900
Log W_t	0.9421	0.03653	25.794	2.92E-87	0.8703	1.0139

Table 3. Regression Analysis Summary for Pitch Moment of Inertia I_y

Regression Statistics	
Multiple R	0.97824
R Square	0.95696
Adjusted R Square	0.95653
Standard Error	0.03952
Observations	407

ANOVA

	Df	SS	MS	F	Signif. F
Regression	4	13.9551	3.4888	2234.29	5.06E-273
Residual	402	0.6277	0.0016		
Total	406	14.5828			

	Coefficients	Standard Error	t Stat	P-value	Lower 95%	Upper 95%
Intercept	-2.0024	0.06439	-31.097	5.07E-109	-2.1290	-1.8758
Log I	1.5315	0.06253	24.493	9.81E-82	1.4086	1.6544
Log T_w	0.2526	0.11272	2.241	2.56E-02	0.0310	0.4742
Log H_r	0.1009	0.05223	1.931	5.42E-02	-0.0018	0.2035
Log W_t	1.0206	0.02950	34.600	1.34E-122	0.9627	1.0786

Table 4. Regression Analysis Summary for Yaw Moment of Inertia I_z

Regression Statistics	
Multiple R	0.98230
R Square	0.96491
Adjusted R Square	0.96456
Standard Error	0.03398
Observations	407

ANOVA

	Df	SS	MS	F	Signif. F
Regression	4	12.7663	3.1916	2763.89	7.27E-291
Residual	402	0.4642	0.0012		
Total	406	13.2305			

	Coefficients	Standard Error	t Stat	P-value	Lower 95%	Upper 95%
Intercept	-1.7797	0.05537	-32.140	3.92E-113	-1.8886	-1.6709
Log WB	1.4316	0.05377	26.624	9.31E-91	1.3259	1.5373
Log TW	0.3811	0.09693	3.932	9.93E-05	0.1906	0.5717
Log RH	0.0188	0.04491	0.418	6.76E-01	-0.0695	0.1071
Log Wt	0.9800	0.02537	38.633	2.11E-137	0.9301	1.0299
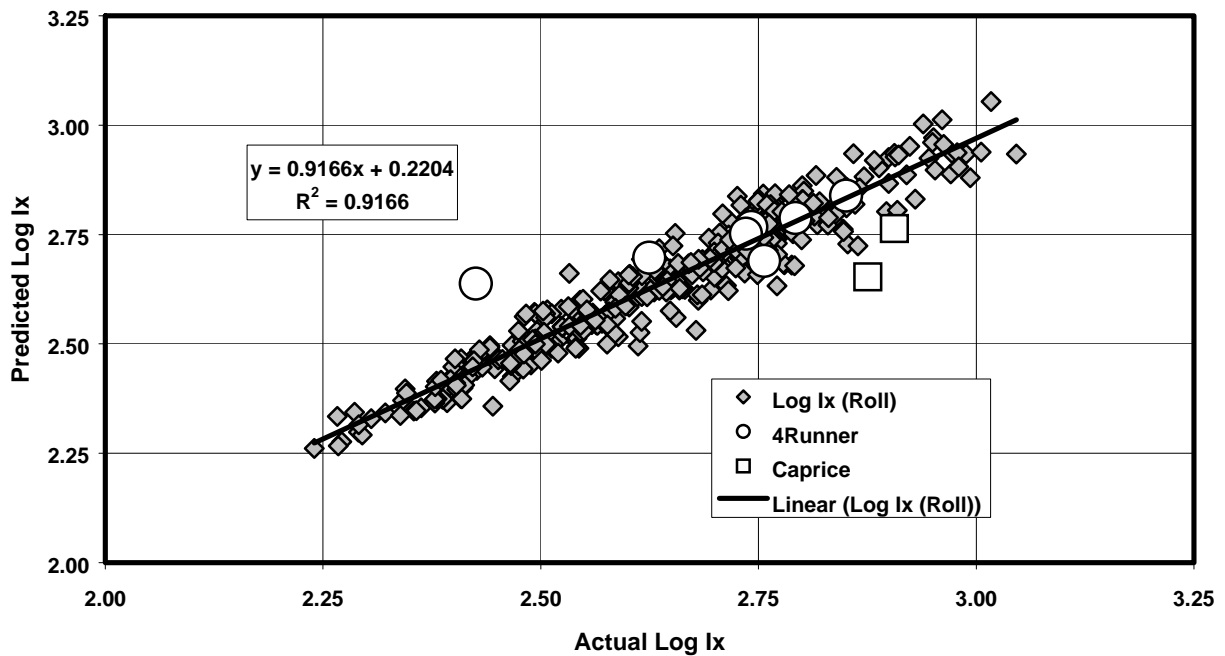
Figure 4. Actual versus Predicted Values of Roll Moment of Inertia (I_x)
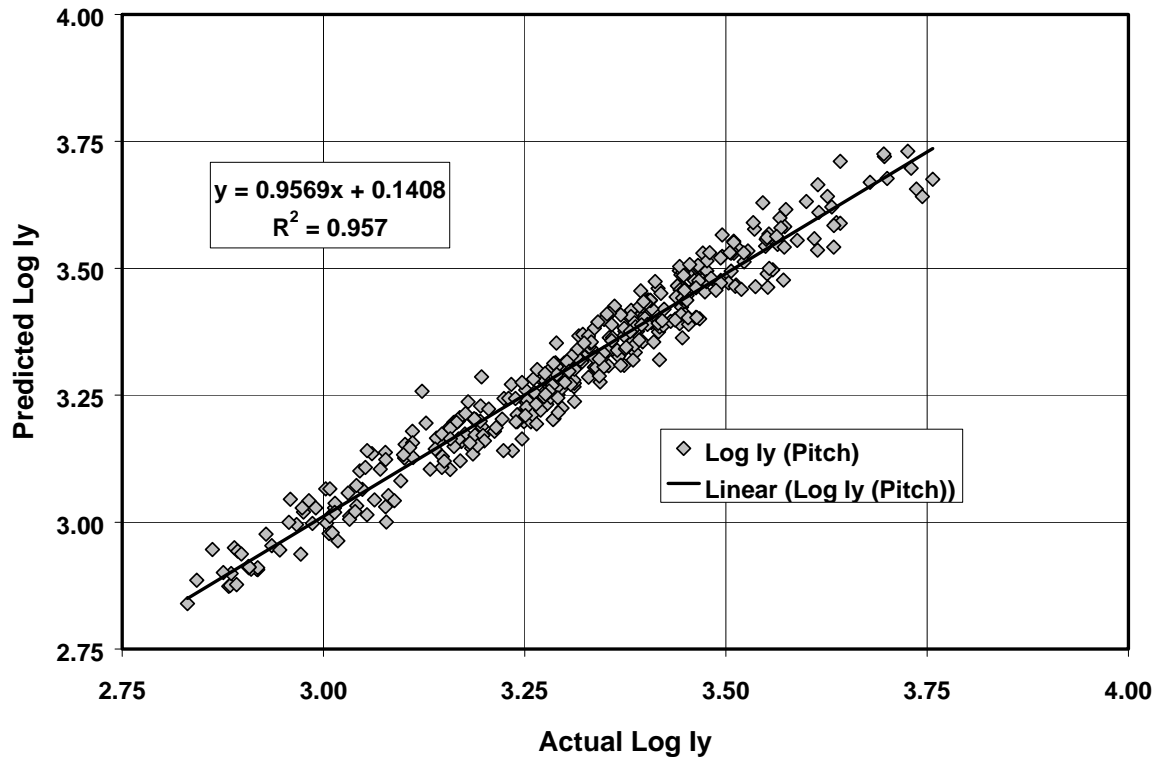
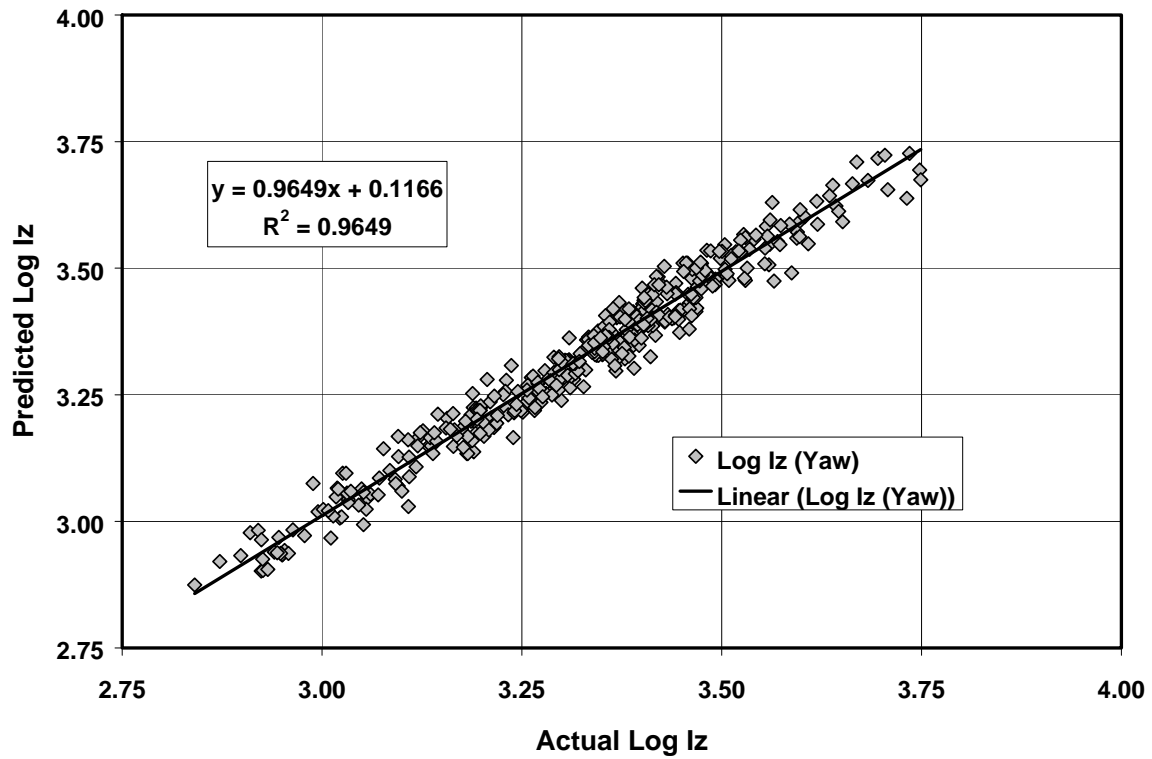Figure 5. Actual versus Predicted Values of Pitch Moment of Inertia (I_y)

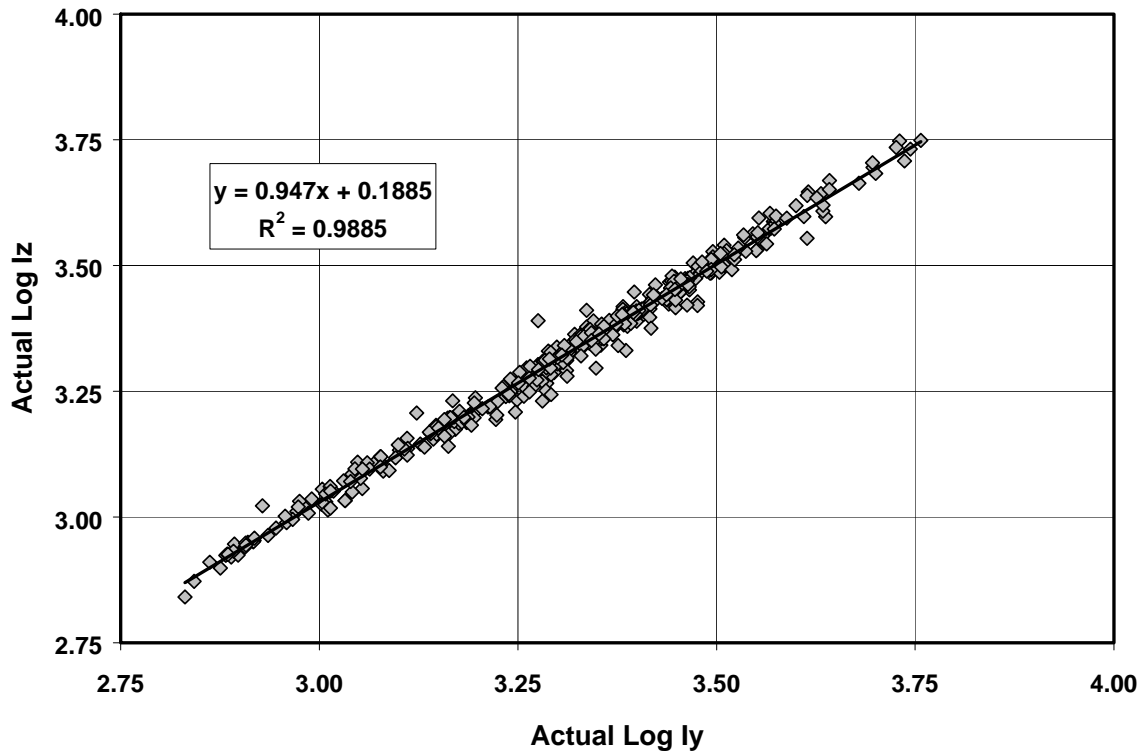Figure 6. Actual versus Predicted Values for Yaw Moment of Inertia

Figure 7. Correlation Between Pitch and Yaw Moments of Inertia

Table 5. Cross Correlation Matrix for Size and Inertial Variables

	Log WB	Log TW	Log RH	Log Wt	Log Ix	Log Iy	Log Iz
Log WB	1.0000						
Log TW	0.7568	1.0000					
Log RH	0.3811	0.5125	1.0000				
Log Wt	0.6639	0.7121	0.6462	1			
Log Ix	0.6793	0.8208	0.6805	0.9231	1.0000		
Log Iy	0.8521	0.7952	0.5953	0.9242	0.9086	1.0000	
Log Iz	0.8571	0.8052	0.5860	0.9268	0.9056	0.9942	1.0000
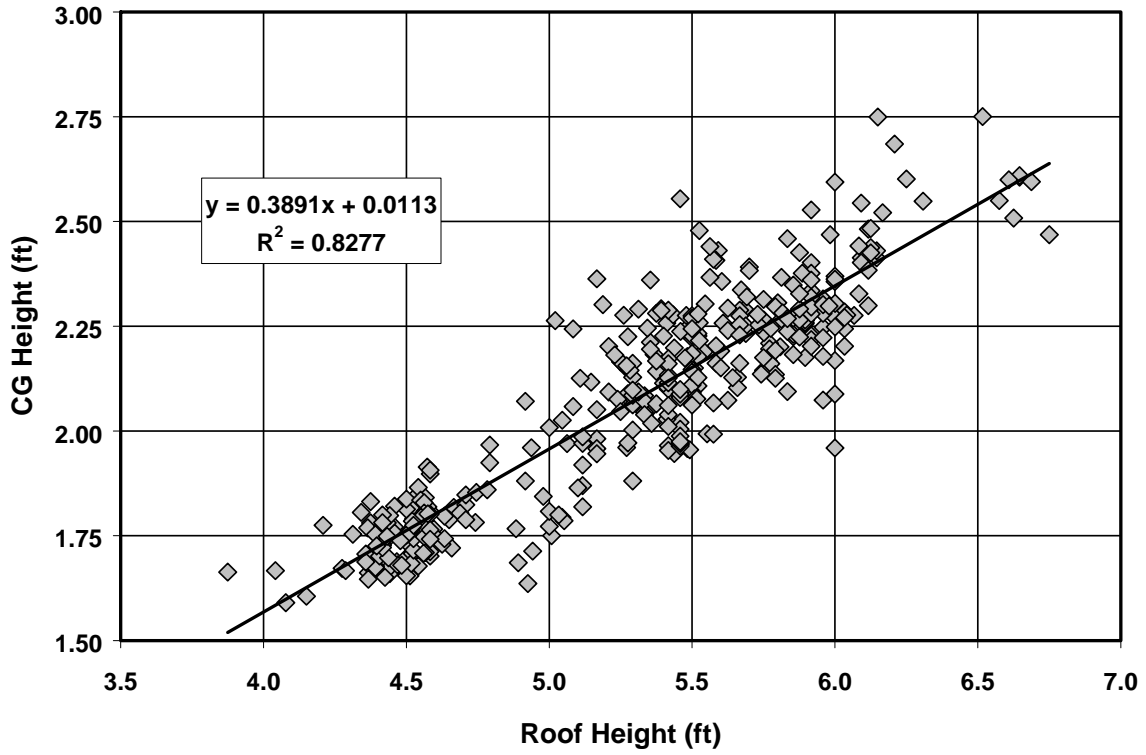
Figure 8. Center of Gravity Height as a Function of Roof Height
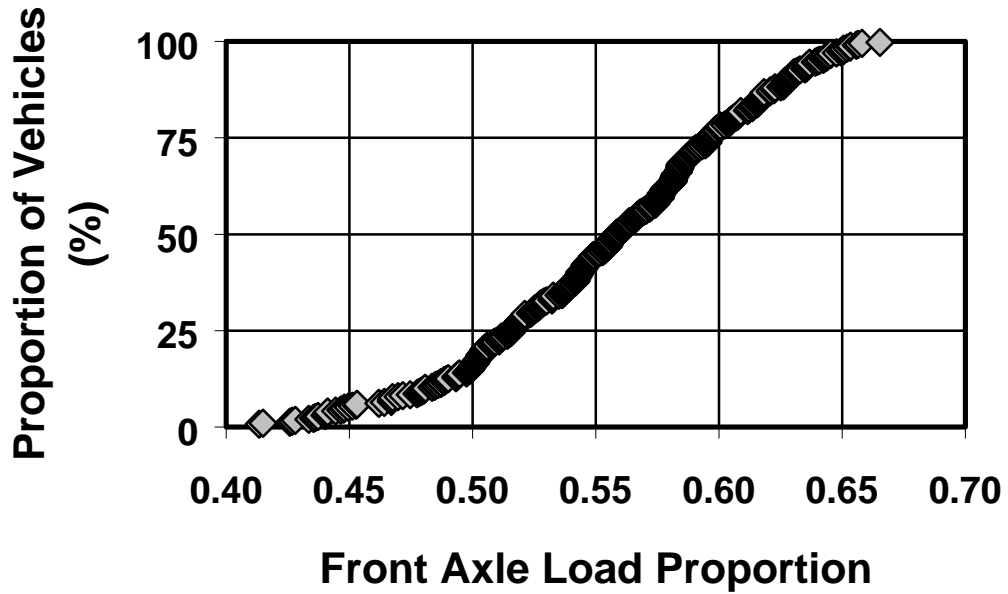

Figure 9. Distribution of Vehicles According to the Proportion of
Front Axle Weight Distribution

$F_c \cong \sqrt{2}mg$ and the radius e was assumed to be given by the distance from the center of gravity to the tire patch. These approximations account for vehicles tipping up in the region of 0.85 and 0.90 g's. Figure 10 shows a plot of the divergence time constant as a function of I'_x / mg. Here we see that large vehicles (i.e. high I'_x / mg) have long divergence time constants, while small vehicles (low I'_x / mg) have shorter divergence time constants. The correlation is high, and the remaining variability is due to the radius e. This analysis suggests that smaller vehicles should tip up faster with other conditions being equal.

COMPUTER SIMULATION ANALYSIS

Computer simulation can be used to explore some of the consequences of the vehicle size relationships developed above. The computer simulation used here has been described previously and has recently been validated for limit performance maneuvers [10]. The computer simulation was used to analyze generic vehicle models meant to characterize small and medium sized SUV's. The vehicle models used in the computer simulation had the general inertial and suspension properties as described in Table 6. As noted the medium sized SUV is about 75% heavier than the small SUV.

Table 6. Example Vehicle Characteristics
Used in Computer Simulation Analysis

Vehicle Characteristics	Generic Example SUVs	
	Small	Medium
Mass (slugs)	82	143
I_{xs} (ft lbs sec)	200	690
I_x (ft lbs sec)	330	1000
I_{ys} (ft lbs sec)	1030	2900
I_y (ft lbs sec)	1200	3200
I_z (ft lbs sec)	1400	2950
mg / I_z	1.89	1.56
I'_x / mg (ft-sec^2)	0.384	0.576
$I'_x = I_{x+}e^2 m$	1,015	2,653
l (feet)	7.22	9.06
T_w (feet)	4.25	5.0
H_{cg} (feet)	1.96	2.31
e (ft)	2.89	3.4
$T_w/2H_{cg}$	1.08	1.08
$T_d = \sqrt{I'_x / \sqrt{2}mge}$ (sec)	0.307	0.346
% Front Roll Stiffness	72	64
% Front Weight	54.2	50.9
Roll Gradient (deg/g)	8.26	8.4
Tire	P205/75R15	P245/70R16

The small vehicle is more sensitive to directional control input and response as characterized by the inertial parameter mg / I_z. The small vehicle also has a smaller divergence time constant (T_d) so that it should tip up quicker. Both vehicles have the same static stability factor ($T_w / 2H_{cg}$) which relates to rollover resistance. The longitudinal center of gravity locations are such that the small SUV has more relative weight on the front axle which should make it more directionally stable. The suspension properties were taken from measurements on real vehicles which resulted in the roll stiffness distributions and roll gradients stated in Table 6. The small vehicle has a higher relative front roll stiffness and slightly lower roll gradient which should also add to its directional stability. The tires for the two vehicles in Table 6 have previously been characterized elsewhere [2, 3].

The steady state response of the two vehicles was determined with the computer simulation by keeping vehicle speed constant and linearly increasing steer angle with time up to the point of limit lateral acceleration. The tire cornering stiffness coefficients (load normalized cornering stiffnesses $Y^*_{\alpha_f}, Y^*_{\alpha_r}$) for each axle were then plotted as a function of lateral acceleration as illustrated in Figure 11. Here we see that cornering stiffness coefficient (CSC) drops off with lateral acceleration as expected as the tires go into saturation. The small SUV starts off with slightly higher CSC's but falls off sooner and saturates at lower lateral accelerations than the medium SUV tires. The higher front roll stiffness distribution and higher front weight distribution of the small SUV have some contribution to these results.

The computer simulation was used to subject the vehicle and tire models to a limit performance steering maneuver consisting of a reversal steering profile which has also been referred to as a fishhook maneuver. This steering profile approximates obstacle avoidance maneuvering, and is a particularly critical maneuver for analyzing rollover propensity due to the severe load transfer and rolling motions that it produces [11]. The maneuver was performed at two speeds, 50 fps (34 mph or 55 kph) and 100 fps (68 mph or 109 kph) in order to consider dynamic speed effects. Maximum steering angles were set to give limit cornering acceleration and the amplitude and timing of the steering profiles were set to be well within the capability of drivers performing emergency maneuvers [4]. Both vehicles had steering ratios of approximately 20 to 1 so that a given steering wheel profile will give an equal front wheel steer angle for both vehicles. At the lower speed, the maximum steering wheel angle was set to 3.5 radians (about 200 degrees) while at the higher speed the maximum steering angle was reduced to 1.5 radians (about 86 degrees) to give limit lateral acceleration conditions [4]. At the beginning of the steering input the throttle was also dropped to approximate the manner in which a driver might respond in an emergency maneuvering situation.
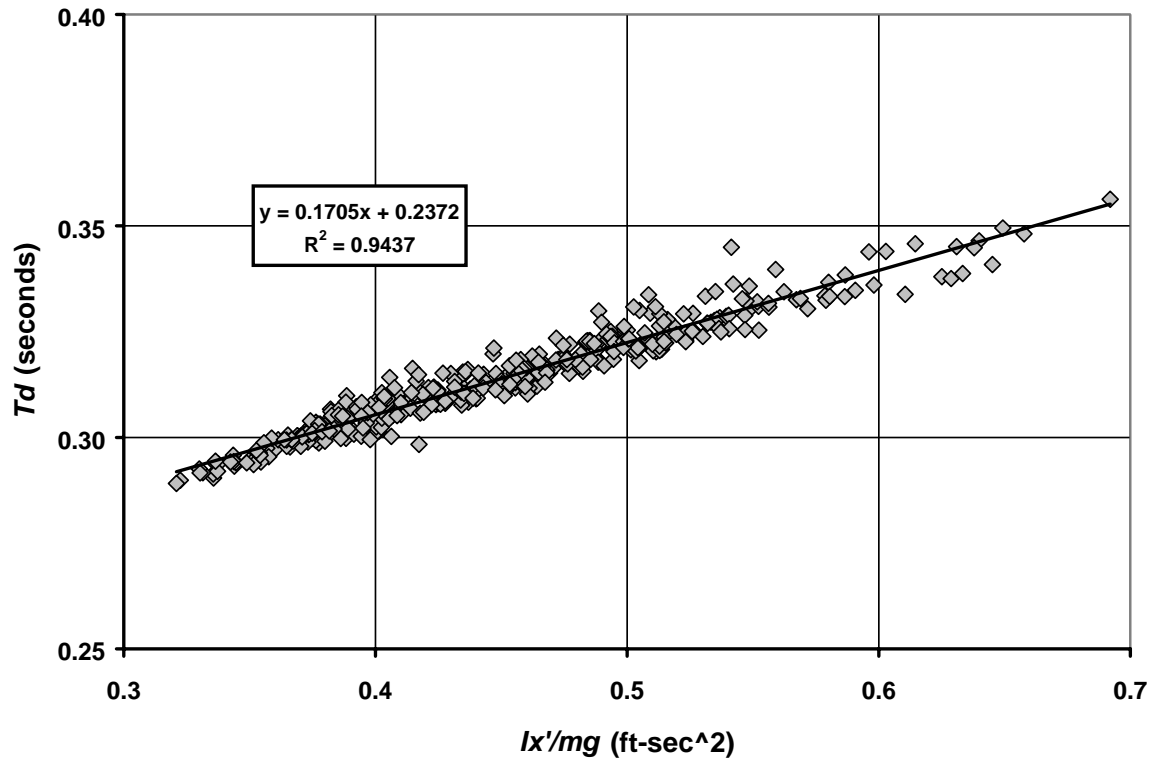
Figure 10. Rollover Time Constant as a Function of the Square Root Roll
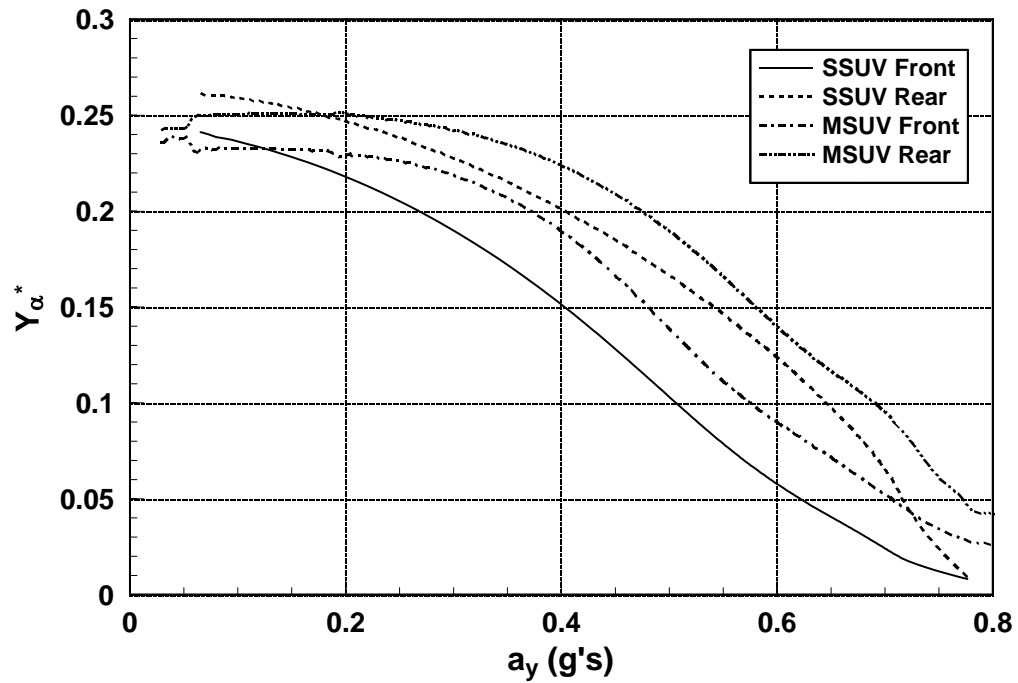Moment of Inertia Divided by Weight

Figure 11. Cornering Stiffness Coefficients as a Function of Lateral Acceleration at the Front and
Rear Axle of a Small Size SUV (SSUV) and Medium Size SUV (MSUV

Time histories for the two SUVs at the two test speeds are shown in Figure 12. All conditions clearly result in tip-ups. Note that once the roll mode becomes unstable, the small size SUV tips up much faster than the medium sized SUV.
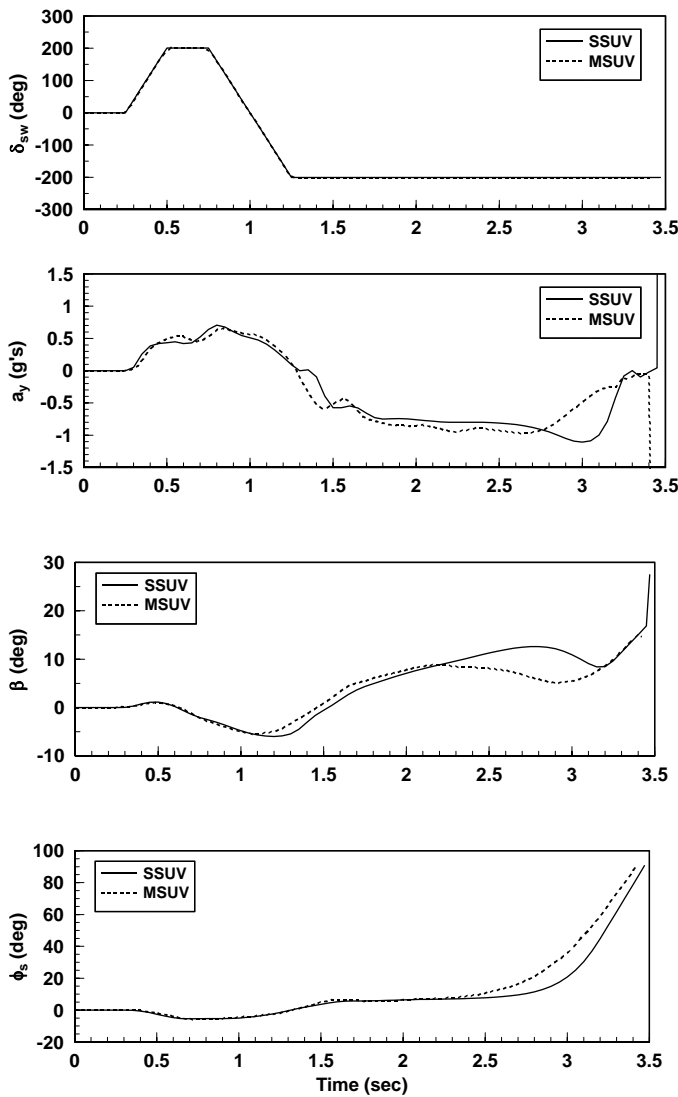
(a) 50 fps Runs
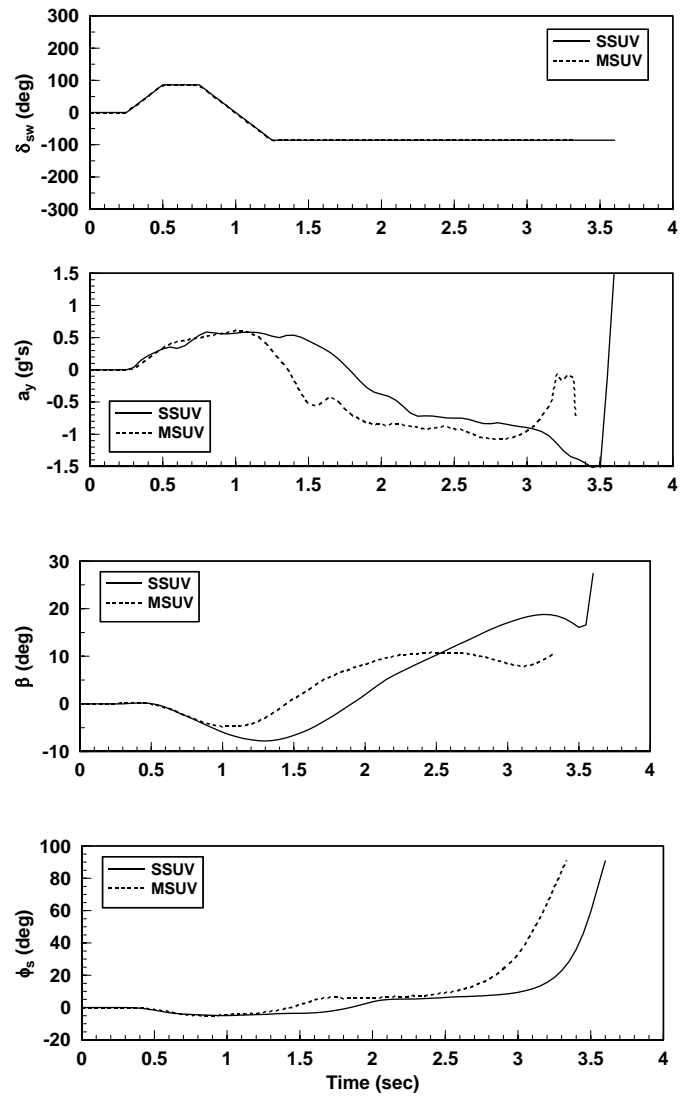
(b) 100 fps Runs

Figure 12. Response of Small and Medium Sized SUVs to a Reversal Steer Maneuver

This is even more strongly portrayed in the Roll Mode Phase Plane plots in Figure 13. Here we see that the dynamics of the roll divergence (instability) are similar in character. The differences are two fold: 1) the medium sized SUV starts its tip-up at a larger roll angle which is consistent with its higher roll gradient; 2) the time constant of the small size SUV is faster than that of the medium SUV as portrayed by the slope of the diverging portion of the phase plane profile.

Figure 14 gives the divergence time constants as identified from the Figure 13 phase plane plots. Here we see that the time constant for the small SUV is almost twice as fast as the medium SUV at the slower speed, and is about 50% faster at the higher speed. The faster roll divergence time constants would make the small

SUV much harder to control under limit performance maneuvering conditions.

The previous rollover instability analysis did not indicate speed to be a factor in the divergence time constant. The dynamic roll gradient plot Figure 15 shows roll angle as a function of lateral acceleration which drives the tip-up instability. The general slope of the cross plot going through the origin is due to the roll gradient, as given in Table 6 for each vehicle, which is the steady state response of roll to lateral acceleration. When lateral acceleration reaches a critical value, something on the order of 28 ft/sec^2 (0.85 g), the roll mode diverges. Note that the smaller vehicle exhibits higher lateral accelerations as do the higher speed conditions. Thus, the composite force quantity in Equation 13 is higher for
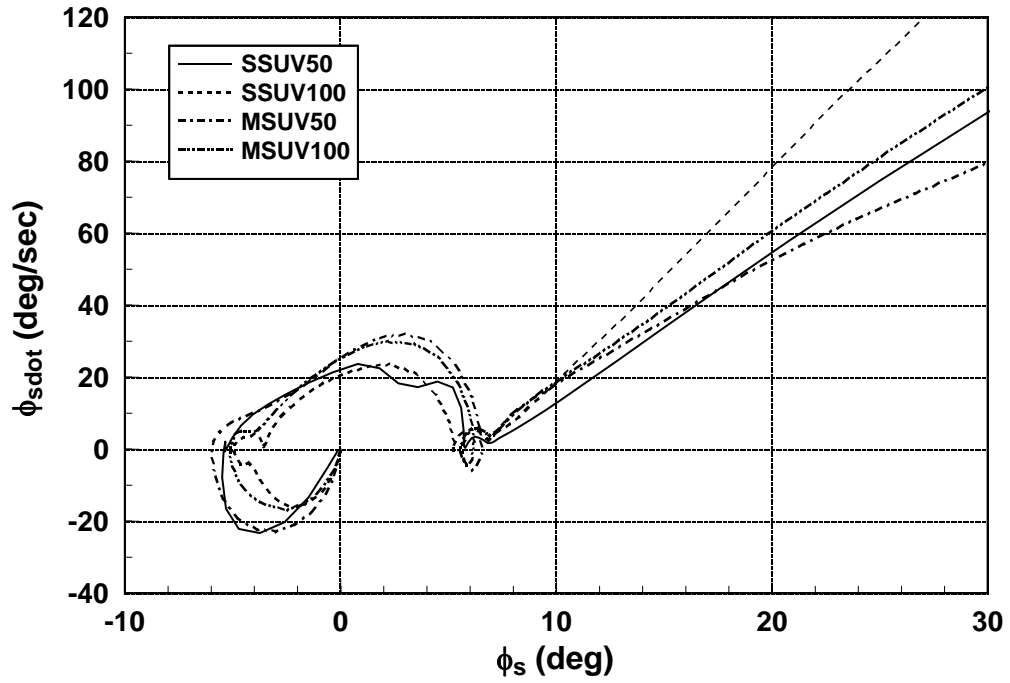
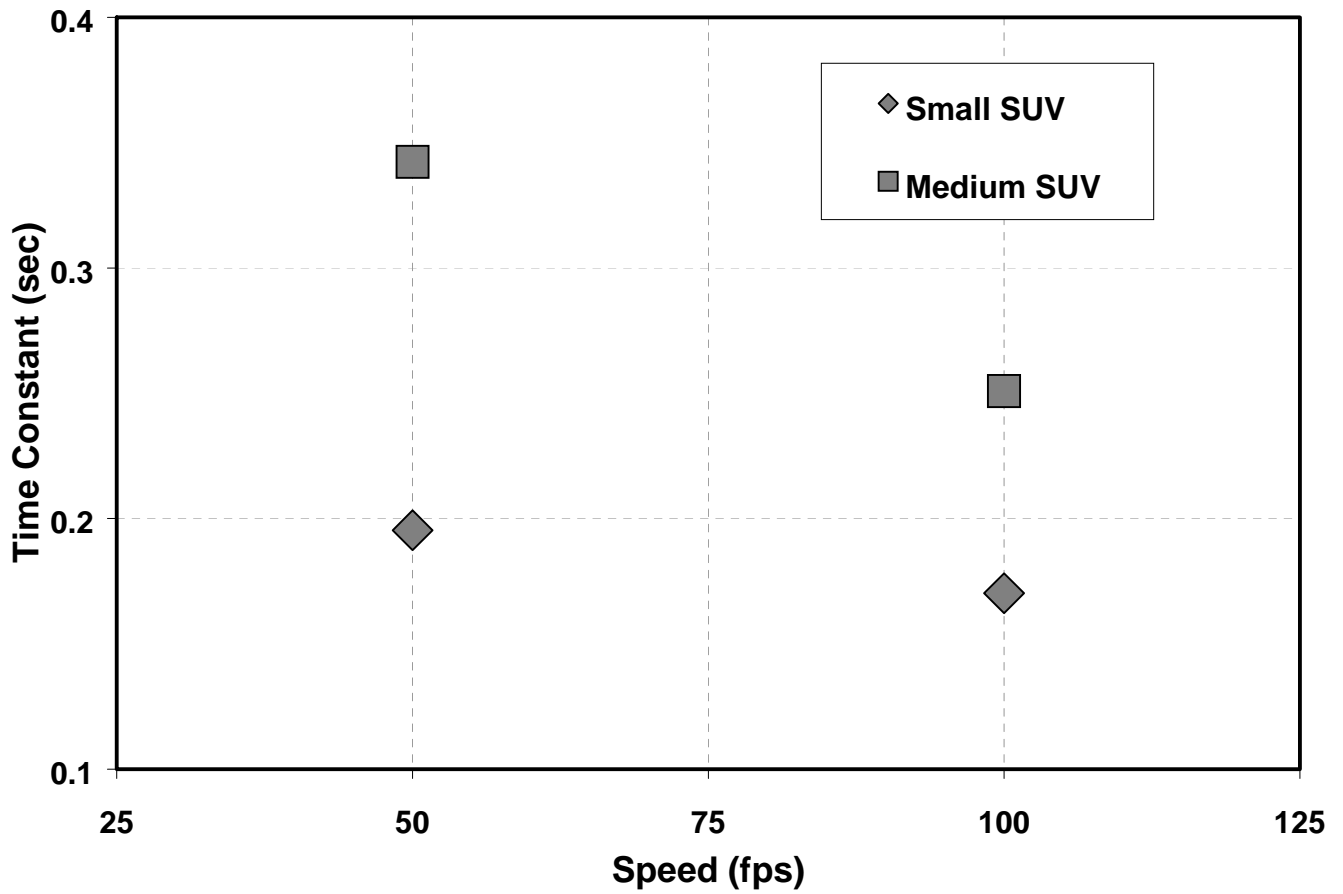Figure 13. Roll Mode Phase Plane Response for Reversal Steer Maneuver

Figure 14. Roll Divergent Time Constants Determine from Computer
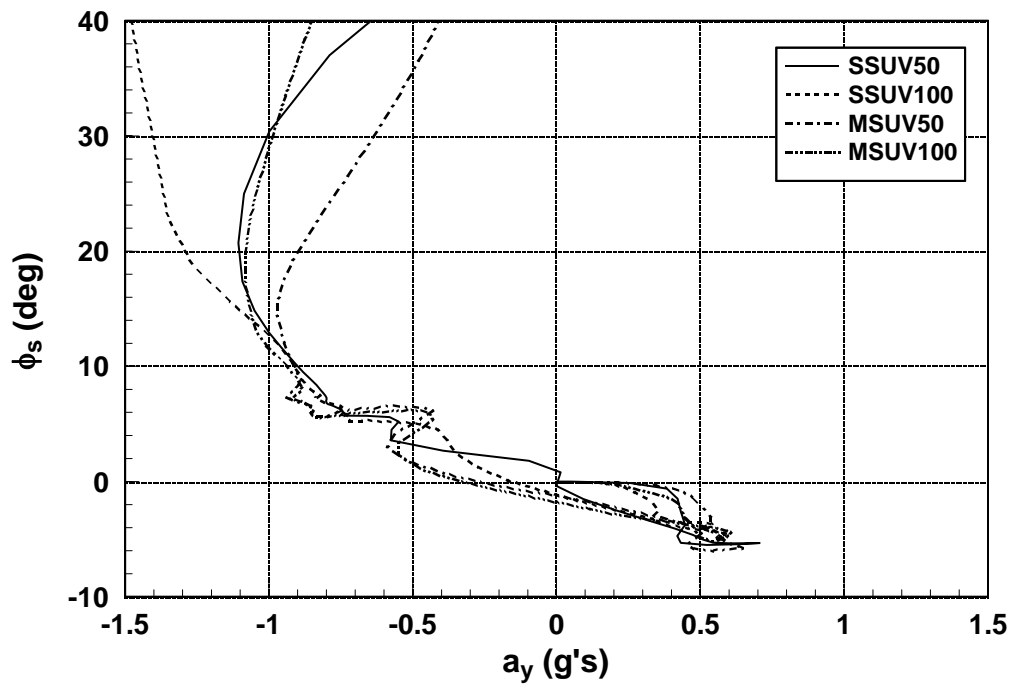Simulation Roll Mode Phase Plane Plots

Figure 15. Roll Angle in Response to Lateral Acceleration

the smaller vehicle and higher speeds. This higher lateral acceleration results in faster tip-up time constants for the smaller vehicle and higher speeds beyond the calculated values shown in Table 6. The directional or yaw mode dynamics of the two SUVs seem to be similar at the 50 fps test speed as illustrated in the directional mode phase plane of Figure 16. However, at 100 fps the dynamics are somewhat different with the small SUV responding with significantly higher yaw rates and side slip angles. The directional mode transient responses in Figure 17 shows the distinctive difference of the small vehicle at the higher speed which is due to its going further into saturation which requires longer to recover during the steering reversal. Also note that both vehicles respond much faster in yaw rate (i.e. a smaller yaw rate time constant) at the lower speed which is consistent with Equation 6.

In a tip-up scenario the directional and roll modes are connected as has been discussed elsewhere [4]. Directional maneuvering causes a vehicle to sustain high side slips which result in high tire side forces and thus high lateral acceleration. The high lateral acceleration then excites the roll mode to tip-up conditions. The interaction of the directional and roll modes are illustrated in the cross plots of Roll Angle versus Body Slip Angle in Figure 18. Here we see that roll angle

divergence starts at some critical body slip angle, then proceeds even as body slip angle decreases. Although the steering profiles are equal for the small and medium sized SUVs, note that the small vehicle reaches larger slip angles, particularly at the higher speed condition.

CONCLUSIONS

The analysis in this paper shows that vehicle inertial properties are strongly correlated with standard measures of length, width and height. It has also been shown that these inertial properties are related to lateral/directional handling and stability.   In particular specific inertial parameters are related to specific dynamic response properties. The ratio of mass to yaw moment of inertia relates to steering sensitivity, which results in small vehicles responding with larger yaw rates than larger vehicles. The ratio of mass to roll moment of inertia relates to the divergence time constant of tip-up. Small vehicles tip up more rapidly than large vehicles because of their smaller ratio of roll moment of inertia to mass. In general, small vehicles respond more quickly and with greater amplitude to steering induced maneuvers which makes them more difficult to control under emergency maneuvering conditions.   These observations appear to be consistent with accident database analyses that show small vehicles more vulnerable to rollover than large vehicles.
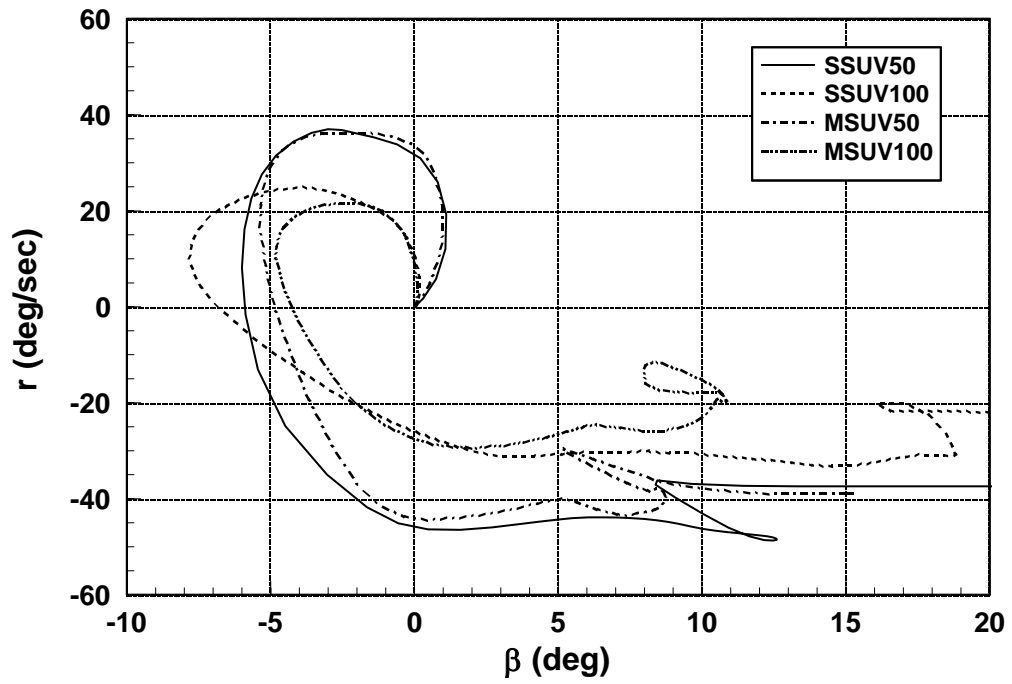
Figure 16. Directional Mode Phase Plane Response for
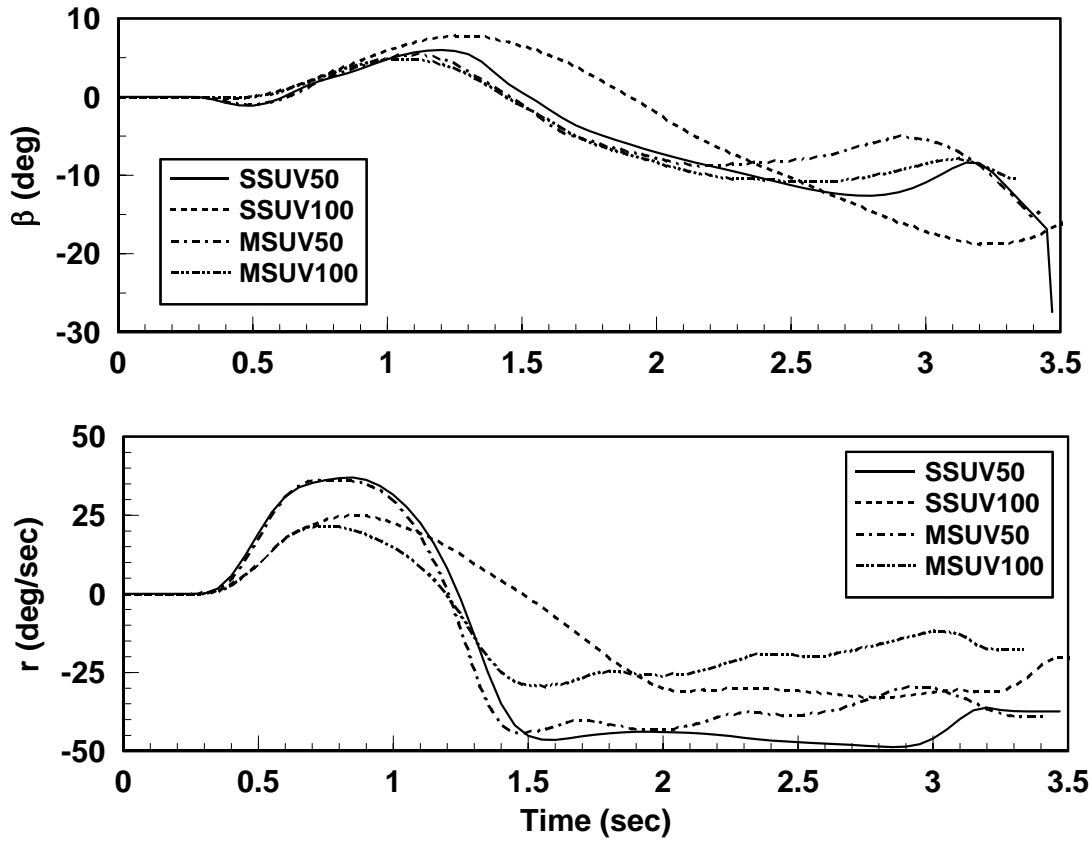OEM Vehicle Reversal Steer Maneuver

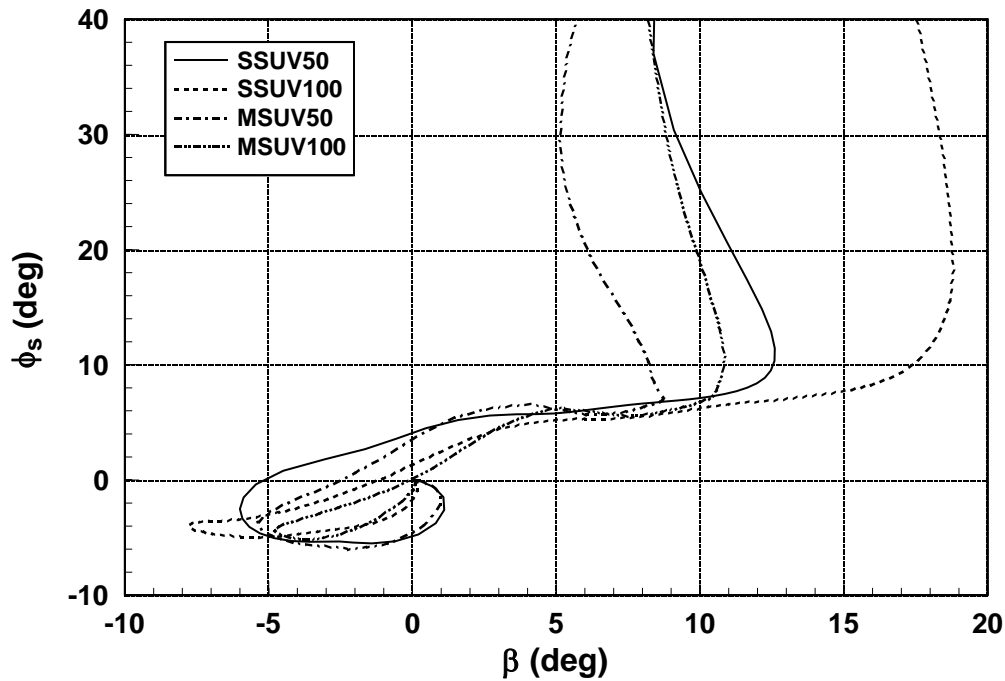Figure 17. Yaw Mode Transient Response

Figure 18. Interaction Between Directional and Roll Modes

REFERENCES

1. Heydinger, G.J., Bixel, R.A., et al., "Measured Vehicle Inertial Parameters-NHTSA's Data Through November 1998," SAE Paper 1999-01-1336, Society of Automotive Engineers, Warrendale, PA, March 1999.

2. Allen, R.W., Myers, T.T., et al., "The Effect of Tire Characteristics on Vehicle Handling and Stability," SAE Paper 2000-01-0698, March 2000.

3. Allen, R.W., Rosenthal, T.J., et al., "The Relative Sensitivity of Size and Operational Conditions on Basic Tire Maneuvering Properties," SAE Paper 2002-01-1182, Society of Automotive Engineers, Warrendale, PA, March 2002.

4. Allen, R.W., Rosenthal, T.J., et al., "Computer Simulation Analysis of Light Vehicle Lateral/Directional Dynamic Stability," SAE Paper 1999-01-0124, Society of Automotive Engineers, Warrendale, PA, March 1999.

5. Allen, R.W., Szostak, H.T., et al., *Vehicle Dynamic Stability and Rollover*, DOT/NHTSA HS 807 956, National Highway Traffic Safety Administration, Washington, DC, June 1992.

6. Mengert, P., Salvatore, S., et al., "Statistical Estimation of Rollover Risk," US Dept. of Transportation/National Highway Traffic Safety Administration Report DOT-HS-807-466, August 1989.

7. Committee for the Study of a Motor Vehicle Rollover Rating System, *The National Highway Traffic Safety Administration's Rating System for Rollover Resistance, An Assessment*, Special Report 265, Transportation Research Board, National Research Council, National Academy of Sciences Press, Washington, D.C., 2002.

8. Allen, R.W., Szostak, H.T., et al., *Analytical Modeling of Driver Response in Crash Avoidance Maneuvering: Vol. I: Technical Background*, DOT-HS-807 270, April 1988.

9. Allen, R. Wade, Rosenthal, T.J., Klyde, D.H. and Chrstos, J.P., "Vehicle and Tire Modeling for Dynamic Analysis and Real-Time Simulation," SAE Paper No. 200-01-1620, SAE Automotive Dynamics and Stability Conference, May 15-17, 2000 Also In: SAE Transactions Journal of Passenger Cars – Mechanical Systems, Vol. 109, 2000.

10. Allen, R.W., Chrstos, J.P., et al., "Validation of a Non-Linear Vehicle Dynamics Simulation for Limit Handling," *Proc. Of the Institution of Mechanical Engineers*, Part D: Journal of Automobile Engineering, Special Issue on Vehicle Dynamics, 2002 vol. 216 No. D4.

11. Allen, R.W. and Rosenthal, T.J., "A Computer Simulation Analysis of Safety Critical Maneuvers for Assessing Ground Vehicle Dynamic Stability," SAE Paper 930760, Society of Automotive Engineers, Warrendale, PA, March 1993.

Nomenclature

a, b = front and rear longitudinal distances between the tire axles and the cg

a_{y_p} = peak lateral acceleration

B, C = quadratic coefficients in bicycle model characteristic equation

e = roll plane diagonal distance from c.g. to tire patch

F_c = composite force through c.g. in roll plane during tip-up

F_z = tire vertical load

g = acceleration due to gravity

H_{cg} = center of gravity height

$I_x \ I_y, \ I_z$ = roll, pitch and yaw moments of inertia

$I'_x = I_x + e^2 m$ = roll moment of inertia about tire patch

$k_z = \sqrt{I_z / m}$ = radius of gyration about the body z-axis;

K = lateral/directional stability factor

K_{LT} = combined tire/suspension lateral compliance

K_{SAE} = (deg/g) = SAE understeer / oversteer gradient

K_ϕ = roll compliance

l = vehicle wheel base

m = total vehicle mass

N_{δ_w} = yaw response to steer response

N_r = yaw stability derivative

r = transient yaw rate

RR = rollovers/single vehicle accident

s = Laplace transform variable

SSF = $T_w / 2 H_{cg}$ = static stability factor

T_r = yaw rate time constant

T_w = track width

U_0 = steady state vehicle forward speed;

u = transient forward velocity

v = transient lateral velocity

W_t = total vehicle weight

Y_v = lateral velocity stability derivative

$Y_\alpha = dF_y / d\alpha$

$Y_\gamma^* = Y_\gamma / F_z$

$Y_\alpha = dF_y / d\alpha$

$Y_\gamma = dF_\gamma / d\gamma$

$Y_\alpha^* = Y_\alpha / F_z$ = non dimensional tire cornering stiffness

Y_{δ_w} = lateral acceleration response to steer input

$Y_{\alpha_1}, Y_{\alpha_2}$ = Front and rear (dimensional) tire cornering stiffnesses.

$\alpha = \tan^{-1}\left(v / u\right)$ = tire lateral slip angle

δ_w = front wheel steer angle